

## Article

# Analysis on Ancient Bloomery Ironmaking Technology: The Earliest Ironmaking Evidence in the Central Plains of China Was Taken as the Research Object

Shuoyang Li <sup>1</sup>, Yanxiang Li <sup>1</sup>, Rong Zhu <sup>2</sup> and Hongyang Wang <sup>2,\*</sup>

<sup>1</sup> School of Institute of Cultural Heritage and History of Science & Technology, University of Science and Technology Beijing, Beijing 100083, China; nengyuanxi@xs.ustb.edu.cn (S.L.); liyanxiang@metall.ustb.edu.cn (Y.L.)

<sup>2</sup> School of Metallurgical and Ecological Engineering, University of Science and Technology Beijing, Beijing 100083, China; zhurongustb1201@163.com

\* Correspondence: whysteel2060@163.com

**Abstract:** The slag found in Hengdong Jiangxian County, Shanxi Province has been recognized by archaeologists as the earliest evidence of bloomery ironmaking in China. The slag was characterized and analyzed by chemical titration, inductively coupled plasma atomic emission spectrometry (ICP-AES), X-ray diffraction (XRD), scanning electron microscopy coupled with energy dispersive spectrometer (SEM-EDS), and tescan integrated mineral analysis (TIMA). The smelting technology in ancient China was explored, combined with thermodynamic theory. The results of chemical titration shown that the total Fe was as high as 64.18%, which means that it was very difficult to produce iron on a large scale with the ancient bloomery ironmaking technology, consuming a lot of iron ore while producing very little iron. The distribution of FeO was relatively dispersed, while that of Fe<sub>2</sub>O<sub>3</sub> particles was concentrated and large. The source of Fe<sub>2</sub>O<sub>3</sub> in the slag can be roughly identified as the oxidized metallic iron, which could not be separated in the slag in the past. Tescan integrated mineral analysis (TIMA) images show that Fayalite and Wustite are the main phase forms in smelting slag. The existence of fayalite proves that the temperature of a slag system should reach the condition of liquid phase formation during the smelting process. Based on the characterization results, the metallurgical conditions of the slag at that time are inferred by FactSage7.1. The theoretical smelting temperature was between 1150 °C and 1200 °C. The fayalite and aluminosilicate in the slag had obvious displacement and inhomogeneity, which pointed to the forging temperature ranging from 1050 °C to 1100 °C.

**Keywords:** bloomery ironmaking slag; ancient ironmaking technology; thermodynamic investigation



**Citation:** Li, S.; Li, Y.; Zhu, R.; Wang, H. Analysis on Ancient Bloomery Ironmaking Technology: The Earliest Ironmaking Evidence in the Central Plains of China Was Taken as the Research Object. *Metals* **2022**, *12*, 1307. <https://doi.org/10.3390/met12081307>

Academic Editor: Man Seung Lee

Received: 22 June 2022

Accepted: 1 August 2022

Published: 3 August 2022

**Publisher's Note:** MDPI stays neutral with regard to jurisdictional claims in published maps and institutional affiliations.



**Copyright:** © 2022 by the authors. Licensee MDPI, Basel, Switzerland. This article is an open access article distributed under the terms and conditions of the Creative Commons Attribution (CC BY) license (<https://creativecommons.org/licenses/by/4.0/>).

## 1. Introduction

The study of ancient block ironmaking technology only through the metallographic structure of unearthed iron ware has great limitations for examining both samples and testing methods [1]. Although the slag is a by-product of mineral smelting activities, its chemical composition, physical phase, and composition of inclusions, contain a large amount of metallurgical technology information, and can provide important physical information for the study of ancient mineral smelting technology.

Bloomery ironmaking technology was the earliest ancient artificial ironmaking method. At the softening temperature of iron ore, the process of directly reducing iron oxide in iron ore to iron by using charcoal or CO as a reducing agent is called the direct reduction method or lump refining method, and its slag is referred to as lump iron refining slag [2]. In addition, blast furnace ironmaking is conducted at a higher temperature. With mainly gas CO and other reducing agents separated from the iron ore in the reduction of iron from

the oxide to liquid metal iron, pig iron is produced by an indirect reduction process. Called the pig iron smelting method, the slag is referred to as pig iron slag [3].

The direct reduction bloomery smelting method generally has a low smelting temperature (about 1100 °C) and no flux is added; most of the iron oxides in the form of complex compounds cannot be reduced and remain in the slag, and the extraction efficiency is very low. The microstructure of a slag matrix is generally mainly forsterite, a small amount of glass phase, sometimes residual metal iron and so on [4]. Due to the low smelting temperature, most of the reduced metal iron is solid ferrite, and droplet liquid metal particles are occasionally seen.

Blakelock combined the archaeological experimental data with the testing results of unearthed cultural relics to analyze the molten slag contained in iron articles. It was considered that the composition of molten slag in ironware was most closely related to the smelting slag produced by smelting [5], but it was difficult to determine the specific smelting process and the type of iron ore because of the difference in lining, fuel and flux. Eliyahu-Behar analyzed the slag and residual iron blocks unearthed from three Iron Age sites in Israel (Hazor, TelBeersheba and Rehov) by means of portable X-Ray fluorescence (XRF), Fourier transform infrared spectroscopy (FTIR) and SEM-EDS [6]. It was demonstrated that all stages of ironmaking at that time, including smelting, refining and forging, were carried out in the city center. The production scale was very small, and it was possible to use a small pit furnace for smelting; a large number of trials have been carried out. In order to further study the furnace type and furnace reaction mechanism of bloomery ironmaking, Workman went into the experiment of simulated smelting, and analyzed the slag and lining produced by simulated smelting by means of portable XRF, Fourier-transform-infrared-spectroscopy and SEM-EDS. It was considered that the lowest curing temperature in these furnaces was about 1100–1115 °C [7]. Theeraporn Chuenpee studied the ancient ironmaking slag at the Ban Khao Din Tai site in northeastern Thailand [8]. The overall chemical composition of the sample was determined by energy dispersive fluorescence spectrometer (ED-XRF). The microstructure and phase composition of the sample were identified by a polarizing microscope and SEM-EDS, and the mineral composition of the sample was further determined by XRD. It was determined that all samples were metallurgical slag produced in blast furnace ironmaking or via a direct smelting process. They all shared very similar chemical compositions, indicating that these samples were produced using similar smelting technologies. Iron, silicon dioxide, and alumina are the main components of most iron smelting slags. No flux was used in the smelting process. According to the presence of iron olivine in all samples, the smelting temperature is determined to be 1100 °C. Li Yanxiang's research team studied the slag in Daye area of Hubei Province. The chemical composition of the slag was determined by WD-XRF and the phase was judged by SEM-EDS. It was demonstrated that the smelting process was bloomery ironmaking rather than pig iron smelting [9]. The team also investigated the ironmaking site in Liucheng (Pingnan County, Guangxi Zhuang Autonomous region, China). The chemical composition of the slag was determined by SEM-EDS, and it was determined that the smelting furnaces were all small shaft furnaces [10].

Thus, it can be seen that researchers have verified the ancient iron smelting methods from the study of the composition and microstructure of the slag. The main characterization methods are XRF, SEM-EDS and XRD. These are semi-quantitative representations. In previous studies, the characterization of slag was mostly concerned with the chemical composition of slag, and the slag was quantified by XRF or energy spectrum. In this case, only the iron content of the slag can be known. However, the specific valence state of iron cannot be fully understood, the  $\text{Fe}^{2+}$  and  $\text{Fe}^{3+}$  in the slag cannot be distinguished, and a thermodynamic model cannot be established to analyze the possible smelting process according to the reduction process of iron oxide. Cavallini has carried out archaeological ironmaking experiments and expresses that the introduction of a thermodynamic model is helpful to understand the chemical reactions taking place in the experimental archaeological metallurgical furnace [11]. However, this paper only lists the iron oxides forming

different valence states and the relationship between the change of standard free energy of CO and CO<sub>2</sub> and temperature, but does not draw the phase diagram according to the slag composition.

On the basis of previous studies, the slag collected from the cultural layer of the Hengdong site is characterized. In addition to being characterized by chemical titration, XRD, ICP-AES, and SEM-EDS, the phase composition of typical samples was detected by Tescan Integrated Mineral Analysis (TIMA) technology. After determining the elemental content and physical phases in the slag, thermodynamic calculations were performed in combination with Factsage 7.1 software (Thermfact/CRCT, Montreal, Quebec, Canada and GTT-Technologies, Aachen, Germany) [12], and phase diagrams were drawn to speculate on the smelting temperature and possible smelting technology available at that time. The slag found at the Hengdong block ironmaking site provides valuable material for the study of the bloomery ironmaking technology in the Central Plain of China.

## 2. General Situation of the Site

The site is located in the northeast of Hengdong Village, Hengshui Town, Jiangxian County, Shanxi Province, with an area of about 100,000 square meters. The whole relic is located on a high platform at an altitude of 572 m, and the west, north and east face alluvial ditches, as shown in Figure 1.

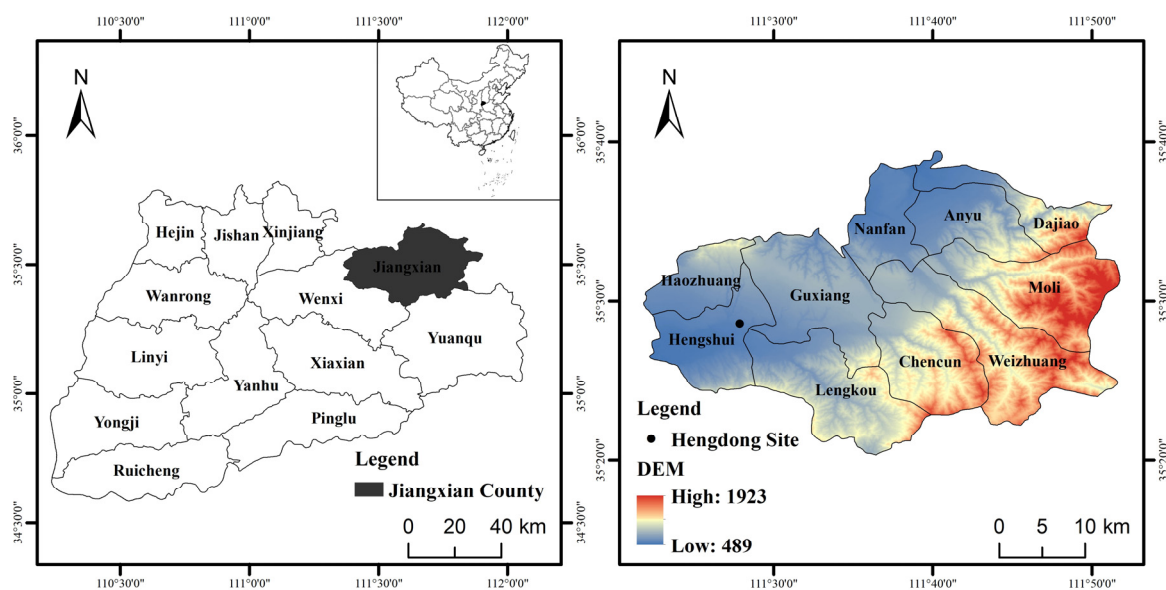


**Figure 1.** Schematic diagram of the location of Hengdong site.

Based on the pottery pieces in the strata of the site, it was concluded that the age of the site is no later than the middle of the Western Zhou Dynasty, and it is the earliest bloomery ironmaking site found in the core area of the Central Plains (Southern Shanxi) [13].

Only one ash pit was found in the whole site. However, the cultural layer is rich, and the local cultural relics department previously investigating determined that the main body of the site was the remains of the Western Zhou Dynasty, and the cultural appearance was relatively single. A total of 10 pieces of slag were recovered from the cultural layer on the western side of the site, small in size, the largest piece being only 2–3 cm in diameter. These slags are black and irregular, magnetic, with one displaying rust, as shown in Figure 2. The sections are mostly black, in crystalline form. From the morphological presentation of the collected samples, it can be roughly determined that the collected slags had undergone a high-temperature process and that liquid phase flow occurred during smelting.

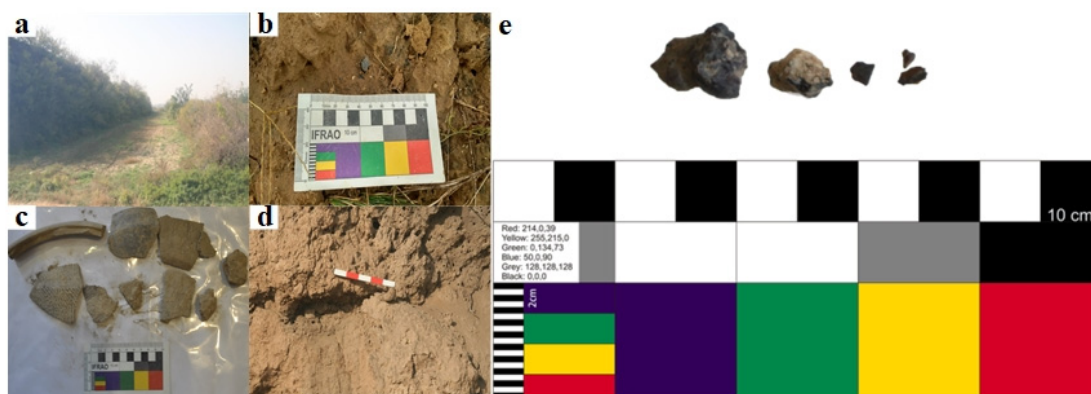


**Figure 2.** General situation of the site and slag samples. (a) Prospect of Hengdong site (b) Ash pit of Hengdong site (c) Pottery pieces in the ash pit (d) Slag in the cultural layer of Hengdong site (e) Sample appearance.

### 3. Quantitative and Characterization Methods

The sample needed to be cleaned thoroughly before testing to avoid soil pollution in the environment and causing analysis error. In order to make the characterization results representative and to give an accurate picture of the composition and structure of the samples, the 10 pieces of slag collected were evenly cut into two parts, thus giving 20 samples. Ten of the 20 samples were used for SEM-EDS analysis. The remaining 10 samples were manually crushed to 200 mesh, which was limited by the sample quality and size, and the samples were prepared by hand. A natural agate mortar with high corrosion resistance and hardness was used to grind the samples in order to avoid the mixing of impurities in the mortar with the material being ground during the grinding process. The remaining samples were crushed and mixed thoroughly, and then divided into 2 parts evenly by mass. One part was used for chemical composition analysis and one part was used for XRD analysis. After crushing, the slag could represent the composition and structure of all slags due to the homogeneous mixing.

#### 3.1. Quantitative Method

The titration method [14] and ICP-AES can accurately quantify the composition of a sample. Bloomery ironmaking technology is equivalent in principle to modern direct reduction iron smelting technology but is limited by low smelting technology and high iron content in the slag, which can be recycled as grade iron ore. In view of this, the analytical detection standard of iron ore and direct reduced iron can be used to detect this batch of ancient slag samples. The content detection method strictly complied with National Standard of the China. In the process of dissolving slag samples, hydrochloric acid was used to prevent  $\text{Fe}^{2+}$  from being oxidized to  $\text{Fe}^{3+}$ .

The total iron content was determined according to the standard of Iron ores, the determination of total iron content using Titanium (III) chloride reduction potassium dichromate titration methods (routine methods). Determination range (mass percentage): 25–72% (ICS:73.060.10, GB/T 6730.65-2009).

The  $\text{Fe}^{2+}$  content was determined according to the standard of Iron ores, the determination of iron (II) content using the potassium dichromate titrimetric method. Determination range (mass percentage): 0.700–30.00% (ICS: 73.060.10, GB/T 6730.8-2016).

The metallic iron was determined according to the standard of direct reduced iron, the determination of metallic iron content using the potassium dichromate titrimetric method after decomposition of the sample by ferric chloride. Determination range (mass percentage): 0.150–3.00% (ICS:73.060.10, GB/T 6730.6-2016).

Mass fraction of carbon or sulfur was determined according to the standard of Iron ores, the determination of carbon and sulfur content, using high frequency combustion with

infrared absorption method. Determination range (mass percentage): carbon 0.01–2.5%, sulfur 0.001–2.00% (ICS: 73.060.10, GB/T 6730.61-2005).

Mass fractions of Na, Cu and K: Iron ores. Determination of potassium, sodium, vanadium, copper, zinc, lead, chromium, nickel, cobalt elements was performed using inductively coupled plasma optical emission spectrometry. Determination range (mass percentage): Na 0.02–0.4%, Cu 0.001–0.4%, K 0.003–0.4% (ICS: 73.060.10, GB/T 6730.76-2017).

Mass fractions of Mg, Al, Ca, P, Si: Iron ores. Determination of aluminum, calcium, magnesium, manganese, phosphorus, silicon and titanium content was performed using inductively coupled plasma atomic emission spectrometric method. Determination range (mass percentage): Mg 0.010–3.00%, Al 0.020–5.00%, Ca 0.010–8.00%, P 0.013–2.00%, Si 0.10–8.00% (ICS:73.060.10, GB/T 6730.63-2006).

### 3.2. X-ray Diffraction

The phase composition of the sample can be qualitatively analyzed by XRD. In order to ensure the consistency of the test results, the remaining samples after the titration test were analyzed directly. The samples were analyzed by Ultima IV X-ray diffraction analyzer (Rigaku, Japan). Detector: Cu anode, a long fine focus ceramic X-ray, graphite monochromator [15], D/teX-Ultra high-speed detector. The test conditions were as follows: scanning voltage 40 kV, scanning current 40 mA, continuous scanning mode, scanning range ( $2\theta$ )  $10^\circ\sim 90^\circ$ , scanning rate  $10^\circ/\text{min}$ .

### 3.3. SEM-EDS

TESCAN VEGA 3XMU scanning electron microscope (TESCAN, Czech Republic) and Bruker energy dispersive spectrometer (Bruker, German) are used to analyze samples. After the surface of the prepared samples was sprayed with carbon, the micro-area energy spectrum information was collected in multiple places under the same field of view as the metallographic microscope and scanned three times for the average. This avoided the hole defects on the sample. Test conditions: excitation voltage of 20 kV, the working distance of 15 mm, counting time of 60 s.

### 3.4. Tescan Integrated Mineral Analysis (TIMA)

TIMA can obtain the overall shape of the sample and the types, contents, and distribution characteristics of minerals and elements, and the quantitative analysis of mineral composition and structure reaches the micron scale, which has irreplaceable advantages over a traditional metallographic microscope and scanning electron microscope in micro-area information extraction. The main component of the equipment is TESCAN field emission variable vacuum scanning electron microscope MIRA3LMU, with TESCAN automatic mineral analysis system. Test conditions: acceleration voltage 25 kV, working distance 15 mm, current and BSE signal strength are calibrated with a platinum Faraday cup automatic program, EDS signal is calibrated with Mn standard sample. The dissociation mode is used in the test process, and the BSE diagram and EDS data are obtained at the same time. The X-ray count of each point is 1000, the pixel is  $3\ \mu\text{m}$ , and the energy spectrum step is  $9\ \mu\text{m}$ .

## 4. Results and Discussion

### 4.1. Results of Chemical Composition Analysis

The chemical composition of the samples is shown in Table 1. The iron content in the slag was high, the composition was complex and there were many impurity elements. Non-metallic elements included Si, P, and S. The geological survey report showed that the highest iron grade of the local primary iron ore was about 65%, and the iron ore grade was higher [16]. The grade of Total Fe in slag was similar to that of iron ore, and the yield of iron was low. At the same time, the silicon content in the slag was much lower than that of the lump ironmaking slag found in other areas in the same period, and the proportion of  $\text{Fe}^{2+}$  and  $\text{SiO}_2$  ( $\text{Fe}/\text{SiO}_2$ ) was higher. This means that it was very difficult for the ancient

bloomery ironmaking technology to produce iron on a large scale, consuming a lot of iron ore while producing very little iron.

**Table 1.** The composition of all the samples after mixing from Hengdong site, wt %.

T Fe	Fe <sup>2+</sup>	Fe <sup>3+</sup>	M Fe	Cu	Na	Mg	Al	Si	P	S	K	Ca
64.18	43.53	20.28	0.37	0.037	0.34	1.05	3.64	4.76	0.15	0.16	0.19	3.07

T Fe-Total Fe; M Fe: Metallic Fe.

There was a large amount of trivalent iron in the slag. It was difficult to define the source of trivalent iron in this part. At present, there may be some errors when using the total iron content as the inference method of smelting technology [17]. The source of trivalent iron was one of the major interfering factors. The source of Fe<sub>2</sub>O<sub>3</sub> is likely to come from two situations. One is that when the slag is smelted, only a small amount of metal iron is generated from wustite. A large amount of wustite is oxidized for a long time to form Fe<sub>2</sub>O<sub>3</sub>. The second is that a large amount of metallic iron has been formed in the smelting process, and the contribution of trivalent iron comes from the oxidized metal iron in the slag. At present, iron-containing utensils of the same period have been discovered in China, so it could be roughly speculated that the source of this part of iron related to the oxidation of a large amount of metallic iron. The source of trivalent iron directly affected the judgment of the smelting process.

#### 4.2. Mineral Phase Composition

The phase composition can be qualitatively analyzed by XRD combined with chemical composition. Compared with the standard phase card, the result is shown in Figure 3. The composition of the slag phase was complex, mainly composed of Fe, Si, Al, O, S, and other complex compounds combined with each other to form. The test results show that it was mainly composed of goethite, aluminosilicate garnet, and a small amount of iron sulfide. The test results showed that it was mainly composed of goethite [FeO(OH)], sillimanite (Al<sub>2</sub>SiO<sub>5</sub>), aluminum iron (AlFeO<sub>3</sub>) and a small amount of iron sulfide (FeS). Because the amount of intercalated metal in the measured sample was very low, no obvious peak related to metal Fe could be observed in the XRD diffraction pattern. The occurrence of goethite [FeO(OH)] could have been due to the interaction between slag and H<sub>2</sub>O in the environment. The samples had been buried in the wet ash pit for a long time, and the goethite in the slag was in fact transformed from the water-eroded iron ore [18]. However, goethite cannot be used for metallurgical thermodynamic analysis. Since goethite is easily dehydrated when heated a little, goethite cannot exist in a high-temperature smelting environment.

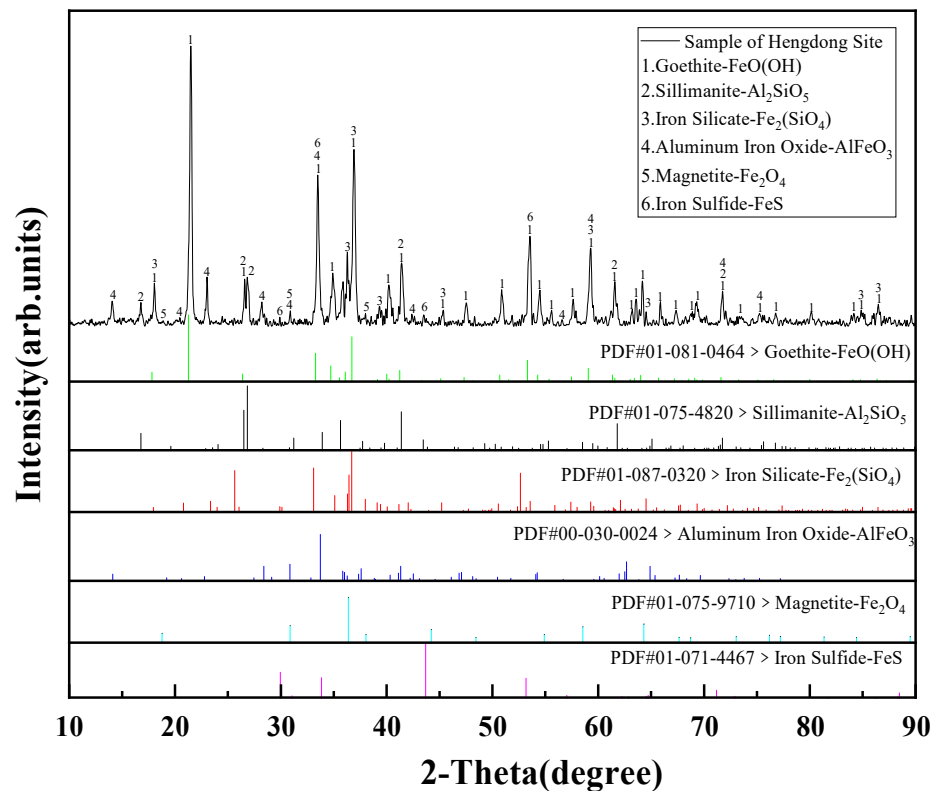
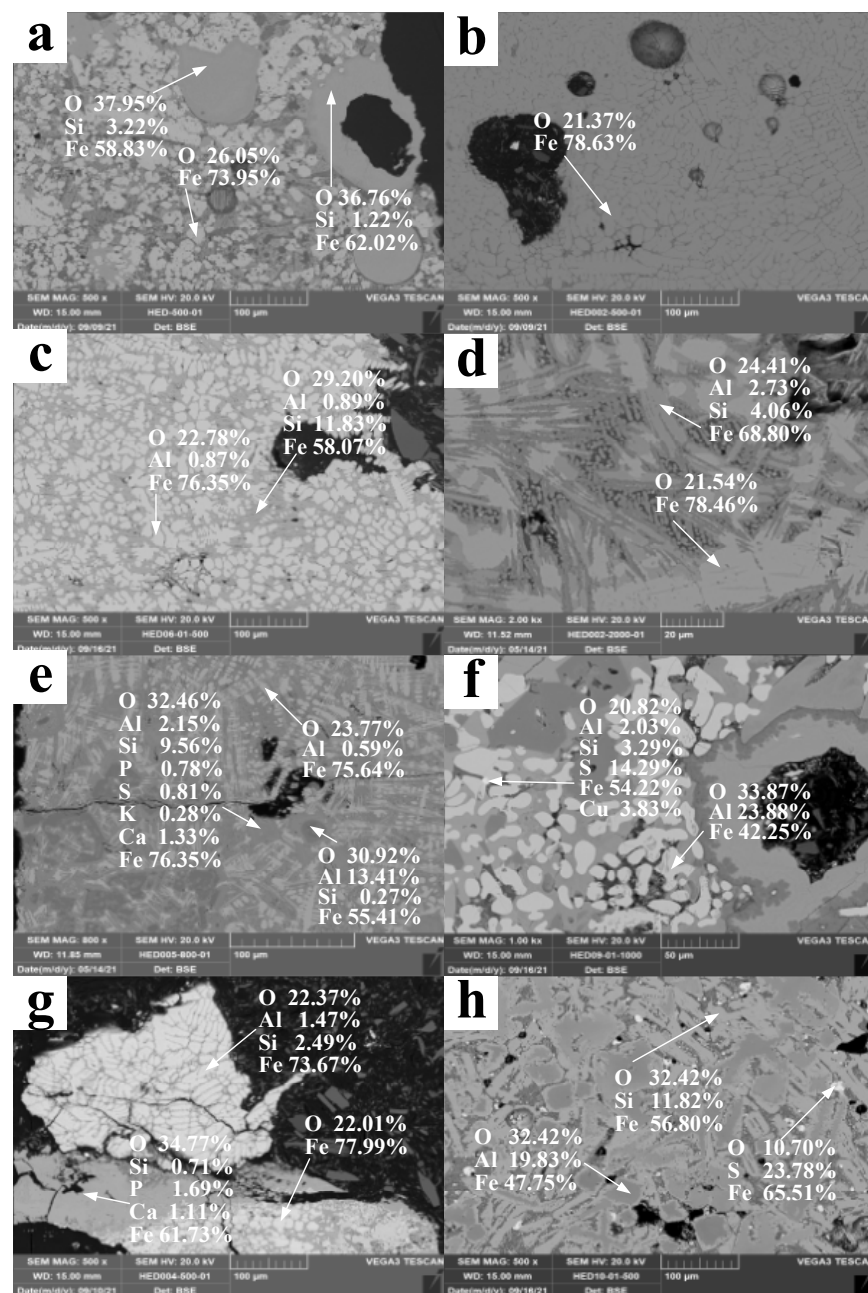


Figure 3. XRD pattern for slags from Hengdong site.

#### 4.3. Morphology of Mineral Phase

The microstructure and phase structure of slag were analyzed by SEM-EDS. The result is shown in Figure 4. The phase structure and distribution characteristics of slag were analyzed by means of surface scanning analysis. They clearly show a brighter wustite and a darker spinel phase, though both of these phases are chemically dominated by Fe and O. It is mainly because the average atomic number of wustite ( $\text{Fe}:\text{O} = 1:1$ ) is higher than spinel ( $\text{Fe}:\text{O} = 3:4$ ). The main form of Fe in the slag was iron oxide, which was evenly distributed in the slag in the form of idiomorph and subhedron. FeS showed bright spots in backscattering mode, intermingled with FeO, and its distribution was relatively scattered.

Obvious particles were found in Figure 4a, and the distribution of  $\text{Fe}_2\text{O}_3$  particles was concentrated and large. The distribution of Hematite is mainly concentrated in the periphery of the hole. The source of this part of Hematite could be roughly determined to be the formation of unseparated metal iron under long-term oxidation. The ancient bloomery ironmaking technology failed to effectively separate the metal iron in the slag, which greatly misled the analysis of the smelting technology of slag. A large number of wustite (FeO) particles were found in Figure 4b. In Figure 4c,d, particles were filled between fayalite ( $\text{Fe}_2\text{SiO}_4$ ) particles. In Figure 4e, the P-containing phase filled the gap between wustite (FeO) particles and spinel particles ( $\text{Fe}_3\text{O}_4$ ). Trace Cu was enriched in FeS particles in Figure 4f. P, containing phase, wustite (FeO), and spinel particles ( $\text{Fe}_3\text{O}_4$ ) were found in Figure 4g. In Figure 4h, a large number of aluminum iron ( $\text{AlFeO}_3$ ) particles had fayalite ( $\text{Fe}_2\text{SiO}_4$ ) at the edge, and a small amount of sulfide (FeS) particles could be detected.



**Figure 4.** SEM photos of slags from Hengdong Site. (a)  $\text{Fe}_2\text{SiO}_4$  and  $\text{Fe}_2\text{O}_3$ ; (b)  $\text{FeO}$ ; (c)  $\text{FeO}$  and  $\text{Fe}_2\text{SiO}_4$ ; (d)  $\text{FeO}$  and  $\text{Fe}_2\text{SiO}_4$ ; (e) P-containing phase filled the gap between  $\text{FeO}$  and  $\text{Fe}_3\text{O}_4$ ; (f) trace Cu was enriched in  $\text{FeS}$  particles; (g) P-containing phase filled the gap between  $\text{FeO}$  and  $\text{Fe}_3\text{O}_4$ ; (h) a large number of  $\text{AlFeO}_3$  particles had  $\text{Fe}_2\text{SiO}_4$  at the edge, and a small amount of  $\text{FeS}$  particles.

#### 4.4. Quantitative Mineral Analysis

In order to further judge the occurrence state of the elements in the slag and to improve the analysis efficiency and scanning accuracy, the representative area was selected for mineral composition and particle size analysis. The result is shown in Figure 5.

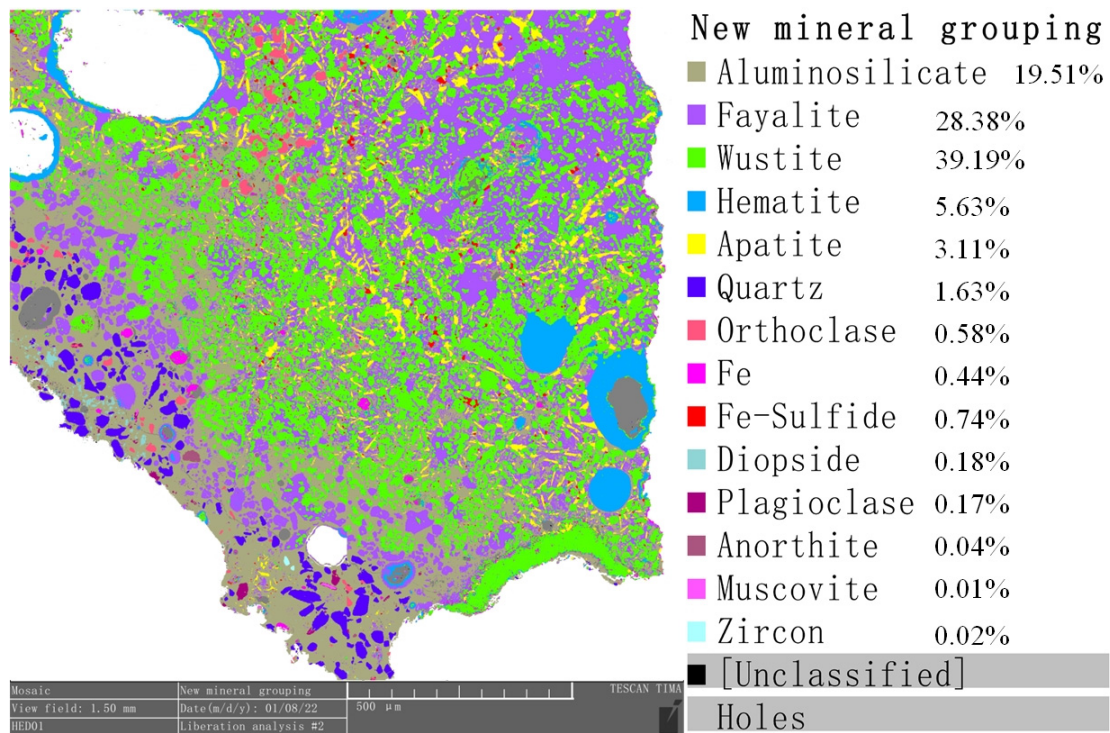


Figure 5. TIMA mineral phases map.

Fayalite and wustite are the main phase forms in smelting slag. Aluminosilicate is evenly distributed in the lower left area of the figure. The presence of Silicate and Fayalite proved that the temperature of the slag system should reach the conditions for the formation of the liquid phase during the smelting process. From the point of view of mineral phase distribution, it can be roughly analyzed that wustite exists in the slag as a solid solution, and the slag system is Fe-Al-Si-O liquid phase. With the decrease in temperature, Fayalite and Aluminosilicate precipitate one after another.

Hematite in slag should be considered as metallic iron, which is the secondary product formed by oxidation for a long time. Metallic iron was found in the sample, and most of the metallic iron is wrapped in Aluminosilicate or around wustite. This result means that in the smelting environment at that time, the reduction conditions provided could satisfy the deoxidation of FeO or iron-containing silicate to form Fe. Apatite becomes the main binding form of P in the slag, and it is dispersed in the slag. Modern smelting technology usually adds CaO combined with direct reduction to solve the problem of phosphorus content in iron ore.

The fluxing material addition technology could not be mastered in ancient smelting, and this part of the source of calcium was attributed to the primary ore. Quartz was found in the Aluminosilicate accumulation area, which proved that the uniformity and stability of the composition could not have been controlled under smelting conditions. Bloomery ironmaking technology involves repeated reduction and forging. In the local area, with the cooling of molten slag, the preferential precipitation of SiO<sub>2</sub> may occur.

#### 4.5. Thermodynamic Analysis in Smelting Process

In order to calculate the thermodynamic properties of slag samples, the composition of slag samples should be studied quantitatively. The Fe<sup>3+</sup> in the slag was caused by metallic iron that could not be separated at that time. Ironmaking is a chemical reaction process with a strong reducing atmosphere. For the characterization of slag in reducing atmosphere, the Fe<sup>3+</sup> in Total Fe should not be considered. Table 2 was obtained by conversion from Table 1, ignoring the influence of P and S, and normalizing after removing Fe<sup>3+</sup>. After percentage normalization, the metallurgical conditions of the slag at that time were predicted. Table 2

shows the composition of slag used in the thermodynamic analysis. Generally, ternary phase diagrams or iso-liquidus phase diagrams were used as a reference for the discussion of ancient smelting technology. Under different oxygen potentials, the liquidus temperature of Fe-Si-O slag system has obvious differences. Table 2 was used as a reference for slag composition, and FactSage 7.1 was used to draw the phase diagram of oxygen potential and temperature. We used the Equilib module calculation in Factsage7.1, and selected databases including Ftoxid, Ftmisc, and FTPS.

**Table 2.** Reference components for thermodynamic calculation.

FeO	Al <sub>2</sub> O <sub>3</sub>	SiO <sub>2</sub>	CaO
72.36	8.89	13.19	5.56

According to the composition of the slag, the equilibrium phase diagram of temperature and oxygen potential was drawn, as shown in Figure 6. In the previous research, there was a lack of analysis of this phenomenon, which simplified the composition of the slag and marked the coordinate points in the ternary phase diagram to obtain the smelting temperature. For example, Charlton marked the composition of lump ironmaking slag in the FeO-SiO<sub>2</sub>-Al<sub>2</sub>O<sub>3</sub> ternary phase diagram drawn in 1964, so as to obtain the temperature of lump ironmaking slag in two different smelting atmospheres [19]. Meng Changwang normalized the FeO, Al<sub>2</sub>O<sub>3</sub> and SiO<sub>2</sub> in the slag matrix, and put the data on the FeO-SiO<sub>2</sub>-Al<sub>2</sub>O<sub>3</sub> slag system diagram. The soft melting temperature of the slag sample was about 1100–1200 °C [20]. Cui Chunpeng depicted the dispersed point of slag directly in the phase diagram of FeO-SiO<sub>2</sub>-Al<sub>2</sub>O<sub>3</sub> system. Judging from the position of scattered point, the temperature range of the ideal melting zone with the lowest temperature is about 1150–1250 °C, which is lower than that of domestic refractories in the same period [21]. Zou Guisen obtained the slag matrix composition by SEM-EDS. After taking the average value, Zou Guisen marked it directly in the FeO-SiO<sub>2</sub>-Al<sub>2</sub>O<sub>3</sub> slag system diagram. It was considered that the average soft melting temperature of the slag sample was about 1150–1250 °C [22]. After summing the average of the slag SEM-EDS analysis results, Huang Quansheng determines according to the FeO-SiO<sub>2</sub>-Al<sub>2</sub>O<sub>3</sub> slag system diagram that the average soft melting temperature of the slag sample without wustite was about 1200 °C, and that of the slag sample with wustite was about 1177 °C [23]. Although the above research could roughly judge the softening temperature of lump ironmaking slag, in the actual smelting process, the composition change of slag from primary slag to final slag is complex, and the phase change of slag is also very complex. Therefore, without considering the oxygen potential and relying solely on the FeO-SiO<sub>2</sub>-Al<sub>2</sub>O<sub>3</sub> ternary slag system, we cannot deeply and accurately understand the changing law of the actual on-site slag, and the slagging system should not be determined only by the primary slag and the final slag. The properties of the intermediate slag are the most important in the iron ore reduction reaction.

On the surface, there are two possible conditions for ironmaking. That is to say, during the slag smelting, there may be lower oxygen potential and smelting temperature, ranging from 1150 to 1250 °C. Alternatively, there can be higher temperature incapable of producing better reducibility in smelting, so that there is no mass production of metallic iron. The analysis of these two cases can be examined from the distribution of wustite. If the molten pool is at a high smelting temperature, then the formation of FeO should be attributed to cooling precipitation; in a large area, wustite should be uniformly distributed. From the results of TIMA, the distribution of wustite shows aggregation. It can be roughly inferred that under the smelting condition, FeO should exist in the slag in the form of solid solution, and the slag is a mixture of wustite and molten slag. It can be roughly judged that the earliest bloomery ironmaking technology in China could not achieve a higher smelting temperature through fuels such as charcoal. At the same time, the oxygen potential between −13~−11 indicates that the bloomery ironmaking technology cannot provide enough CO

gas for the reduction of iron oxides, which lengthens the process for smelting to reduce the oxygen potential of the slag. The liquid phase formation temperature of the phase diagram is similar to that of Vanessa Workman. The sample temperature is below 1050 °C when the slag is completely solidified and ironmaking is completed.

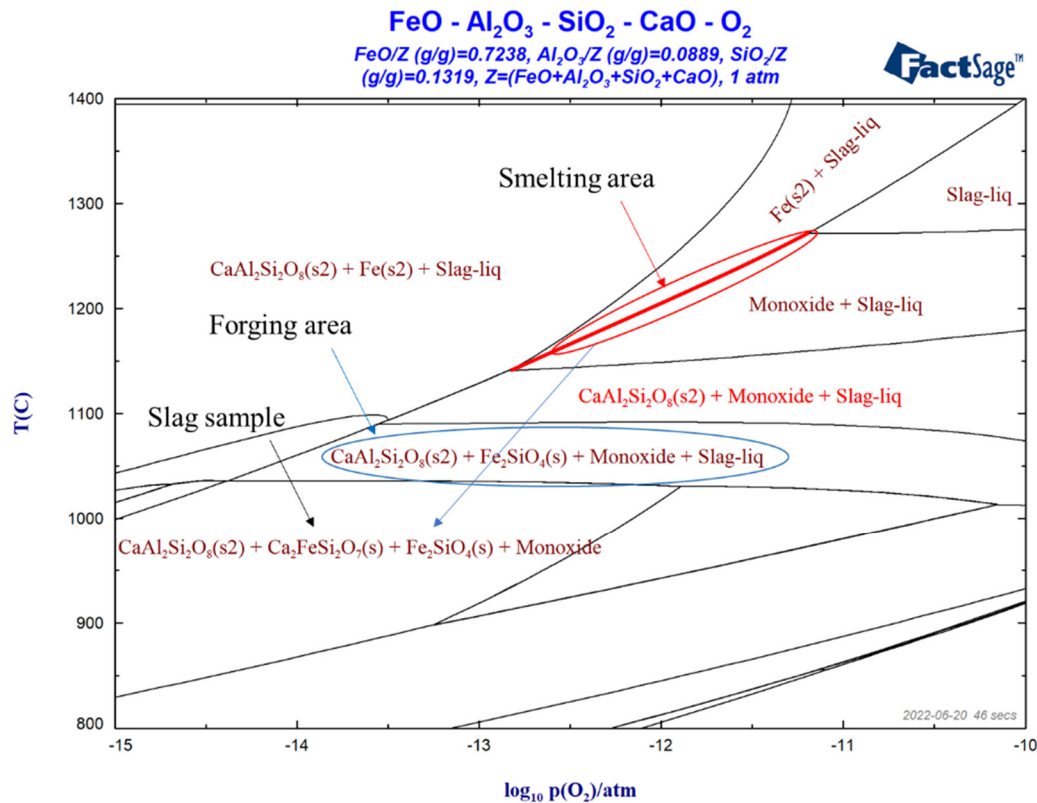


**Figure 6.** Temperature-oxygen potential phase diagram of slag from Hengdong Site.

It can be seen from the TIMA pattern that fayalite shows a flow trend in the slag, which indicates that fayalite may be preferentially precipitated as a solid solution in the forging process of lump ironmaking. The mixed Fe-Ca-Al silicate finally precipitated. From the phase diagram of Figure 6, it can be inferred that the actual operating temperature is between 1050 °C and 1100 °C. It may be because the primary ore contains a certain amount of CaO, which causes the actual smelting temperature to be slightly lower than that of other bloomery ironmaking technologies. When the temperature of the sample is lower than 1050 °C, the slag solidifies completely and ironmaking is complete.

## 5. Conclusions and Significance of the Study

- (1) The development of ironmaking technology is a gradual process, which was the result of the long-term development of high temperature technology system and redox control system. Bloomery ironmaking technology appeared earlier and was widely used in most parts of the East Asia, and there may also have been a stage of using block ironmaking in early China. The age difference of the iron wares unearthed in the tombs of Guo State [24], Liangdai village [25] and Tianma-Qucun in the middle Spring and Autumn period [26] should not have exceed 200 years. The test results of this batch of samples showed that the bloomery ironmaking technology was mastered in the core area of the Central Plains of China in the middle and late Western Zhou Dynasty.
- (2) Under smelting conditions, FeO existed in slag in the form of solid solution, and slag was a mixed liquid of wustite and molten slag. Since a high smelting temperature cannot be achieved through fuels such as charcoal, and sufficient CO gas cannot be

provided for the reduction of iron oxides, the reduction of oxygen potential of slag will have required a long smelting time.

- (3) The sample was bloomery ironmaking slag, and the actual operating temperature was between 1050 °C and 1100 °C. It may be that the primary ore contained a certain amount of CaO, which led to the actual smelting temperature slightly lower than that of the bloomery ironmaking technology in other areas. When the sample temperature was lower than 1050 °C, the slag solidified completely.

**Author Contributions:** Data Curation, methodology, and manuscript review, S.L.; Conceptualization, funding acquisition, and supervision, Y.L.; Funding acquisition and supervision, R.Z.; Formal analysis, writing-review, and editing, H.W. All authors have read and agreed to the published version of the manuscript.

**Funding:** This research received no external funding.

**Institutional Review Board Statement:** Not applicable.

**Informed Consent Statement:** Not applicable.

**Data Availability Statement:** Not applicable.

**Conflicts of Interest:** The authors declare no conflict of interest.

## References

- Buchwald, V.F.; Wivel, H. Slag Analysis as a Method for the Characterization and Provenancing of Ancient Iron Objects. *Mater. Charact.* **1998**, *40*, 73–96. [[CrossRef](#)]
- Tylecote, R.F. A history of metallurgy. *Br. Corros. J.* **1977**, *12*, 137–140. [[CrossRef](#)]
- Siddique, R.; Cachim, P. *Waste and Supplementary Cementitious Materials in Concrete: Characterisation, Properties and Applications*; Woodhead Publishing: Cambridge, UK, 2018.
- Stefanescu, D.M. *ASM Handbook Vol. 1A Cast Iron Science and Technology*; ASM International: Geauga, OH, USA, 2017; pp. 3–11.
- Blakelock, E.; Martín-Torres, M.; Veldhuijzen, H.A.; Young, T. Slag inclusions in iron objects and the quest for provenance: An experiment and a case study. *J. Archaeol. Sci.* **2009**, *36*, 1745–1757. [[CrossRef](#)]
- Eliyahu-Behar, A.; Yahalom-Mack, N.; Gadot, Y.; Finkelsteina, I. Iron smelting and smithing in major urban centers in Israel during the Iron Age. *J. Archaeol. Sci.* **2013**, *40*, 4319–4330. [[CrossRef](#)]
- Workman, V.; Maeir, A.M.; Eliyahu-Behar, A. In search of the invisible hearth: An experimental perspective on early Levantine iron production. *J. Archaeol. Sci. Rep.* **2021**, *36*, 102803. [[CrossRef](#)]
- Chuenpee, T.; Won-In, K.; Natapintu, S.; Takashima, I.; Dararutana, P. Archaeometallurgical Studies of Ancient Iron Smelting Slags from Ban Khao Din Tai Archaeological Site, Northeastern Thailand. *J. Appl. Sci.* **2014**, *14*, 938–943. [[CrossRef](#)]
- Larreina-Garcia, D.; Li, Y.; Liu, Y.; Martín-Torres, M. Bloomery iron smelting in the Daye County (Hubei): Technological traditions in Qing China. *Archaeol. Res. Asia* **2018**, *16*, 148–165. [[CrossRef](#)]
- Zou, G.; Meng, Z.; Li, Y.; Huang, Q.; Cui, C. From bowl furnaces to small shaft furnaces: New evidence from ancient bloomery iron smelting site at Liuzhuoling in Guangxi, Southern China, ca. 400 to 700 AD. *Archaeol. Anthropol. Sci.* **2022**, *14*, 54. [[CrossRef](#)]
- Cavallini, M. Thermodynamics applied to iron smelting techniques. *Appl. Phys. A* **2013**, *113*, 1049–1053. [[CrossRef](#)]
- Bale, C.W.; Bélisle, E.; Chartrand, P.; Decterov, S.A.; Eriksson, G.; Hack, K.; Jung, I.-H.; Kang, Y.-B.; Melançon, J.; Petersen, S.; et al. FactSage thermochemical software and databases—recent developments. *Calphad* **2009**, *33*, 295–311. [[CrossRef](#)]
- Lianghui, Q. A preliminary study of the characteristics of metallurgical technology in ancient China. In *Chinese Studies in the History and Philosophy of Science and Technology*; Springer: Dordrecht, The Netherlands, 1996; pp. 219–241.
- Iwama, T.; Du, C.M.; Koizumi, S.; Gao, X.; Ueda, S.; Kitamura, S.Y. Extraction of phosphorus and recovery of phosphate from steelmaking slag by selective leaching. *Isij Int.* **2019**. ISIJINT-2019-298. [[CrossRef](#)]
- Epp, J. X-ray diffraction (XRD) techniques for materials characterization. In *Materials Characterization Using Nondestructive Evaluation (NDE) Methods*; Woodhead Publishing: Cambridge, UK, 2016; pp. 81–124.
- Wang, A. Types and characteristics of main iron deposits in Zhongtiao Mountain. *Hubei Nat. Resour.* **2011**, 26–27. (In Chinese)
- Thomas, G. *A Chemical and Mineralogical Investigation of Bloomery Iron-Making in the Bristol Channel Orefield, UK*; Cardiff University: Cardiff, UK, 2000.
- Mancini, A.; Lothenbach, B.; Geng, G.; Grolimund, D.; Sanchez, D.F.; Fakra, S.C.; Dähn, R.; Wieland, E. Iron speciation in blast furnace slag cements. *Cem. Concr. Res.* **2021**, *140*, 106287. [[CrossRef](#)]
- Charlton, M.F.; Crew, P.; Rehren, T.; Shennan, S.J. Explaining the evolution of ironmaking recipes—An example from northwest Wales. *J. Anthropol. Archaeol.* **2010**, *29*, 352–367. [[CrossRef](#)]
- Zou, G.; Meng, Z.; Li, Y.; Huang, Q.; Cui, C. Preliminary Study on Metallurgical Relics Unearthed from Liuzhuoling Iron Smelting Site in Pingnan, Guangxi. *Nonferrous Met.* **2022**, *14*, 54. (In Chinese)

21. Cui, C.; Li, Y.; Chen, S.; Xi, Q. A Primary Study on the Smelting Relics in Ezhou, Hubei Province. *Jiangnan Archaeol.* **2016**, *3*, 102–111. (In Chinese)
22. Zou, G.; Li, Y.; Yang, Z.; Gao, C.; Huang, Q. Preliminary Study on Ancient Iron Smelting Site in Datang Village, Huaihua City, Hunan Province. *Nonferrous Met.* **2020**, 92–98. (In Chinese)
23. Huang, Q.; Li, Y. A preliminary study on tieshitang smelting site in Pingnan County, Guangxi. *Sichuan Cult. Relics* **2012**, 92–96. (In Chinese)
24. Wang, Y.; Liu, Y.; Jiang, T.; Chen, K. Scientific Research of Bimetallic Objects Unearthed from M2009 in the Guo State Cemetery at Sanmenxia. *Spectrosc. Spectr. Anal.* **2019**, *39*, 3154–3158. (In Chinese)
25. Chen, J.; Yang, J.; Sun, B.; Pan, Y. Fabrication technology of copper iron complex unearthed from M27 of Liangdai village Site. *Sci. Sin.* **2009**, *39*, 1574–1581. (In Chinese)
26. Han, R. A metallographic study on early iron objects of China. *Wen Wu* **1998**, 1998, 87. (In Chinese)